Multi-Channel SAR Research at the Naval Research Laboratory

Mark Sletten[1], Luke Rosenberg[2], Robert Jansen[1] , Steve Menk[1], Jakov Toporkov[1]
1 - US Naval Research Laboratory, USA
2 - Defence Science and Technology Group, AUSTRALIA

mark.sletten@nrl.navy.mil

ABSTRACT

This paper describes research at the Naval Research Laboratory (NRL) into Multi Channel Synthetic Aperture Radar (MSAR) and features data collected with the NRL MSAR system. The NRL MSAR is an airborne test bed designed to investigate remote sensing and surveillance applications that exploit multiple along-track phase centers, in particular, applications that require measurement of scene motion. The system operates at X-band and supports 32 along-track phase centers through the use of two transmit horns and 16 receive antennas. As illustrated in this paper, SAR images generated with these phase centers can be coherently combined to directly measure scene motion using the Velocity SAR (VSAR) algorithm, and these measurements can then be used to correct the image distortion that the motion causes. This unique radar was deployed in 2014 and 2015, and this paper presents a description of the system and representative results. Also included is a discussion of ongoing efforts to improve the magnitude and phase balance across the 32 channels, as this is essential to effective VSAR processing.

1.0 INTRODUCTION

High fidelity imaging of moving targets is a well-known challenge for synthetic aperture radar (SAR), especially in ocean environments. Standard SAR processing methods assume the entire scene is stationary, and interpret the Doppler histories in the data accordingly. Any Doppler shifts introduced by target or scene motion will be misinterpreted and the corresponding backscatter will be misplaced in the image. The classic example of this is the 'train-off-the-track', in which the signature of a range-traveling train appears displaced from the signature of the track upon which it is running. More serious distortion can occur when vessels roll and pitch on a dynamic ocean surface, causing different parts of the vessel to move at different speeds relative to the SAR.

One approach to this problem is to use a multi-channel SAR system with multiple phase centers arranged along the flight direction. The array of phase centers generates a "time stack" of images from which detailed motion can be detected using the velocity SAR (VSAR) algorithm, originally proposed by Friedlander and Porat [1] [2]. While these motion measurements are useful in themselves for target detection and oceanic studies, they can also be used to correct the image distortion that the motion produces [2]. In [3] and [4], this was demonstrated using a ground-based MSAR test bed, and [8] presents the first reported demonstration using an actual airborne platform, the Naval Research Laboratory Multi Channel SAR (NRL MSAR). In this NATO-SET paper, these airborne results are reviewed and recent investigations related to the balancing of the magnitude and phase across the multiple channels are also summarized. This balancing operation is essential for effective VSAR processing. However, as illustrated below, aircraft multipath makes this balancing operation particularly challenging.

2.0 VSAR MOTION MEASUREMENT AND DISTORTION CORRECTION

Motion of the SAR platform, be it an aircraft or a satellite, is essential for SAR imaging. Coherent backscatter is collected as the platform moves a small antenna past the scene, and the recorded signals are then combined in a SAR processor in order to "synthesize" a much larger antenna and thereby form an image with fine azimuthal resolution. However, motion of scatterers *in the scene* cause image distortion. Radial motion, i.e. motion directed towards or away from the SAR, produces displacements in the cross-range direction, which for a stripmap SAR looking broadside, is also the along-track or azimuth direction. This distortion is unavoidable in any single-channel SAR system, and results from the inability of standard SAR image formation algorithms to distinguish between intended platform motion and unknown motion in the scene itself. Standard SAR processing algorithms assume the scene is stationary, and use the sample-to-sample phase history along the synthetic aperture to precisely determine the cross-range location of the objects that produce the backscatter. Radially-directed scene motion will produce an additional sample-to-sample phase change, but the SAR processor can interpret only the *total* phase progression, so it consequently displaces the object signatures in the azimuth direction. The amount of this displacement is proportional to the Doppler velocity of the object backscatter, v_r , and is given by

$$\delta_a = v_r \frac{R}{V_p} \tag{1}$$

where R is the distance between the SAR platform and the object, and V_p is the platform velocity. Cross-range motion in the scene also induces distortion, but in the form of azimuthal defocusing. For maritime scenes, this distortion component tends to be significantly less severe than the azimuth displacements caused by radial motion.

While a single-phase-center SAR cannot distinguish between platform motion and motion in the scene, an MSAR with its phase centers arranged along the flight direction *can* make this distinction. This is illustrated in Figs. 1 and 2 for the case of a stripmap data collection and an MSAR with M along-track phase centers. As illustrated on the left side of Fig. 1, as the aircraft flies, each phase center collects data along a linear trajectory in space and time. By selecting a synthetic aperture that is common to all M phase centers (see vertical dashed lines), M images of a given area can be formed, as shown in cartoon form on the right of Fig. 1. This group of images is referred to as a time stack. The dark stripe in each image is intended to represent a low-reflectivity road, while the two colored dots represent the signatures of two cars traveling on it. Due to the "train-off-the-track" distortion mechanism, the car signatures are displaced from the road, with the displacement of the faster (red) car being greater than that of the slower (blue) car. By construction, these images all cover an identical area on the ground and share a common vantage point in space. But due to the fact that their corresponding phase centers

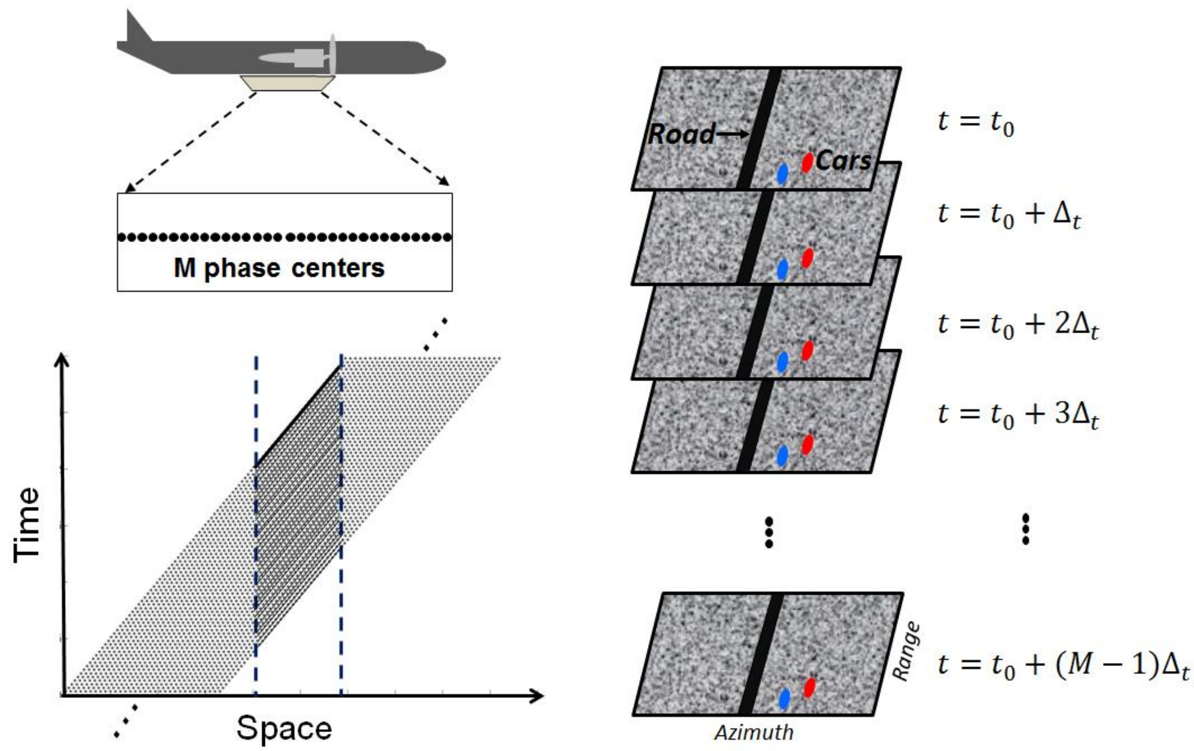

Figure 1. Cartoon showing the formation of an image time stack.

are arranged along the flight direction, there is a progression in effective collection time from one image in the stack to the next. For MSAR systems designed to measure scene motion, this time offset is small (on the order of ms or less), and thus the M *magnitude* images are essentially identical.

However, motion in the scene causes image-to-image changes in the pixel *phase*. SAR images are complex valued, and the phase of a given pixel is proportional to the fine-scale distance between the SAR and the objects producing the backscatter in that pixel. VSAR analyzes the phase progression along the stack in order to extract motion measurements. This is illustrated in Fig. 2 where Doppler processing is performed on each and every pixel in the image to transform the time stack into a velocity stack, in which each image corresponds to different Doppler velocity bin. This velocity stack is simply the Doppler spectra for each and every pixel, arranged by range and azimuth. The two spectra for pixels containing the cars are indicated in the middle of Fig. 2. The Doppler processing is generally performed by means of a Fast Fourier Transform (FFT), although as discussed in [8], more advanced spectral estimators can also be used.

Using the basic properties of the FFT, the velocities corresponding to each of the images in this transformed stack are given by

$$v_m = -v_0 + (m-1)\Delta_v \qquad m = 1 \dots M \tag{2}$$

where

$$v_0 = \frac{f_s}{2}\frac{\lambda}{2} = \frac{\lambda}{\Delta_t 4} = \frac{V_p \lambda}{2d} \quad (3)$$

$$\Delta_v = \frac{f_s}{M}\frac{\lambda}{2} = \frac{\lambda}{\Delta_t M 2} = \frac{V_p \lambda}{dM} \quad (4)$$

and d is the along-track spacing between receive elements, λ is the radar wavelength and $f_s = 1/\Delta_t$ is the Doppler sampling frequency determined by the time interval between the images in the time stack, Δ_t [2].

While the VSAR motion measurements are useful in themselves for scene characterization, they can be used further to correct the train-off-the-track distortions caused by the motion itself. This is depicted on the right side of Fig. 2. Through (1)-(4), the azimuth displacement error of each velocity image is known. These errors can therefore be corrected by simply shifting each velocity image back by this amount. As shown in the cartoon, this corrective shift places the signature of each vehicle in its proper position on the road. To form a single corrected image, the images in the shifted velocity stack can be summed incoherently, as depicted in the lower right in Fig. 2.

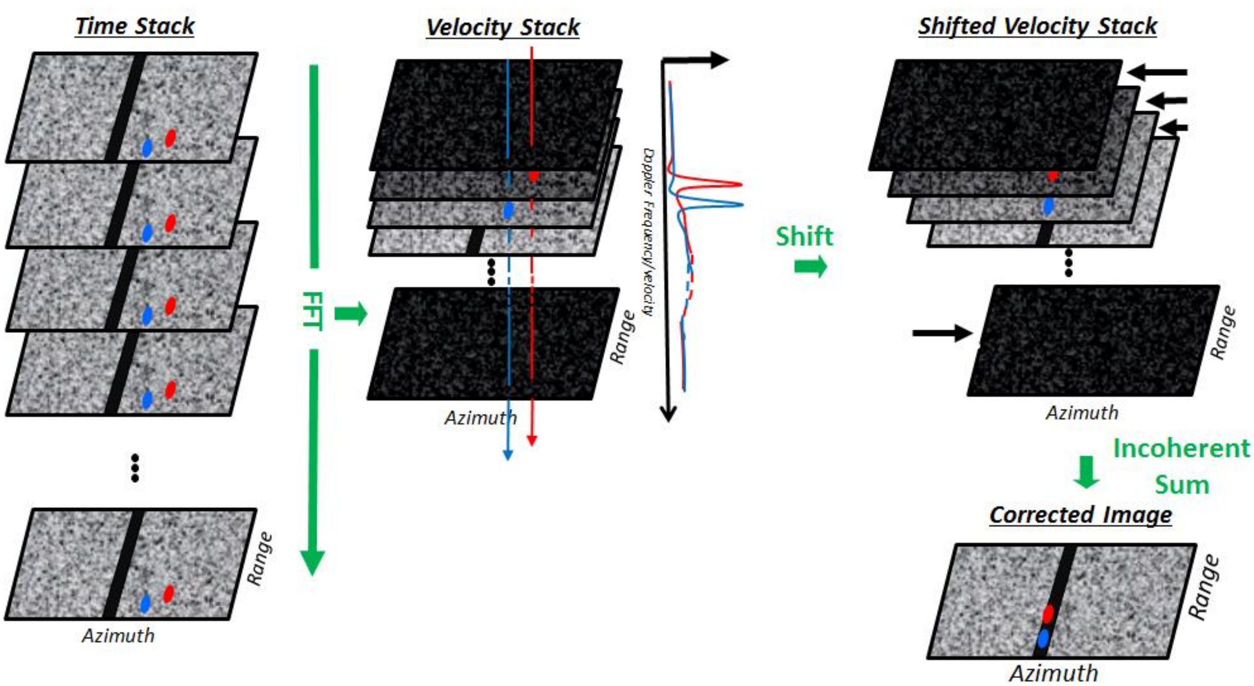

Figure 2. Illustration of the VSAR algorithm. The technique uses Doppler processing to first convert the time stack into a velocity stack. Azimuthal displacements due to scene motion are then corrected by shifting the velocity stack, and a corrected image is formed by incoherently summing the shifted images.

3.0 THE NRL MSAR SYSTEM

The NRL MSAR is an airborne system based on the NRL Focused Phased Array Imaging Radar (NRL FOPAIR), a ground-based MSAR test bed [3]. The MSAR system operates at X-band with a center frequency of 9.875 GHz and uses linear frequency modulated (LFM) chirped waveforms with a bandwidth of 220 MHz to achieve a range resolution of approximately 0.7 m. The peak radiated power is approximately 1.4 kW, while the aggregate pulse repetition frequency (PRF) of 25 kHz and pulse length of 6 μs produce a total average power of 210 W. The system flies on a Saab 340 aircraft using a belly-mounted radome with a nominal depression angle of 20º, as shown in Fig. 3. The MSAR system uses 16 receive antennas, equally spaced along the flight axis with a separation of 10.48 cm, and two transmit horns, with a spacing of 125.8 cm. A photograph of the antennas as installed in the Saab radome is shown in Fig. 4. The long white enclosures below the two transmit horns contain the 16 receive antennas. All antennas are vertically polarized. During odd-numbered pulse repetition intervals (PRIs), the aft-mounted horn transmits, while the fore-mounted horn radiates during even PRIs. During each pair of up-down PRIs, four of the 16 receive antennas are connected to a four-channel receiver and sampled by a high speed data recorder. After each pair of PRIs, a bank of microwave switches is reconfigured to connect the next group of four receive antennas to the receiver and data recorder. After a total of 4 PRI pairs (320 μs), this scan sequence is repeated. In this manner, 32 phase centers are generated, corresponding to each combination of transmit and receive antennas, and are sampled at a per-phase-center PRF of 3.125 kHz. This PRF is sufficient to allow production of 32 SAR images that are free from azimuthal ambiguities. Note that the average power associated with any one of these images is 1/32 of the total average power, or 6.7 W. Since the location of a given phase center is halfway between the corresponding transmit and receive antennas, the along-track spacing between these phase centers is 5.24 cm, half the physical spacing between the receive elements. Note that given the spacing between the two transmit horns, four of the phase centers corresponding to the aft-mounted transmit horn are collocated with four produced by the fore-mounted horn. Thus the total number of independent phase centers is 28 with total length of 141.5 cm.

Figure 3. Saab 340 aircraft with the NRL MSAR radome mounted beneath the fuselage.

The large number of phase centers and the requirement to revisit each frequently enough to allow alias-free SAR imaging produces a high average data rate. During each pulse repetition interval (PRI) of 40 μs, 8192 8-bit samples from each of the 4 data recorder channels are written to a redundant array of independent disks (RAID) for a sustained data rate of 819 MB/s. The recorder is based on a 4-channel, 12-bit acquisition card running at a sample rate of 500 MS/s. Selection of the 8192-sample range window within each PRI and reduction of the 12-bit samples down to 8-bits is performed by a field programmable gate array. Motion of the antennas is measured by a Novatel inertial navigation system mounted in the Saab radome directly behind the antennas. The Novatel ProPak6 OEM638 receiver blends GPS position data with measurements from a Litton LN200 inertial measurement unit to determine the precise positions of all phase centers at a 100 Hz rate. These data are used during image formation processing in order to compensate for non-ideal aircraft motion.

Figure 4. Interior view of the NRL MSAR radome.

4.0 REPRESENTATIVE RESULTS

The NRL MSAR was deployed in 2014 and 2015 over the Outer Banks of North Carolina, on the mid-Atlantic coast of the USA. This area was selected for flight testing due to the wide variety of potential moving targets, including vehicles, boats, tidal currents, and shoaling waves.

Fig. 5a shows an uncorrected NRL MSAR image of Oregon Inlet, southeast of Elizabeth City, NC, and the bridge that spans it. To improve contrast, 16 original SAR images, one from each of the up-chirp images, were incoherently added to form the image. For comparison, Fig. 5b contains the corresponding VSAR-corrected image, formed by incoherently summing the 16 shifted (i.e. corrected) velocity images. The images contain five faint echoes produced by cars travelling on the bridge, as highlighted by the red and blue ovals. In the original, uncorrected image, all five echoes are displaced from the bridge, with one displaced to the left, produced by a northbound vehicle, and five displaced to the right, produced by southbound cars. All five signatures are brought back to the bridge through VSAR processing. VSAR also places the signals produced by vessels back at the head of their signatures, as indicated by the green ovals. (The vertical streaks bracketing the bridge are range sidelobes produced by the high reflectivity of the bridge supports.) The faint automobile signatures are much more apparent in 5c, where the image has been colorized based upon the dominant velocity, as described in [8].

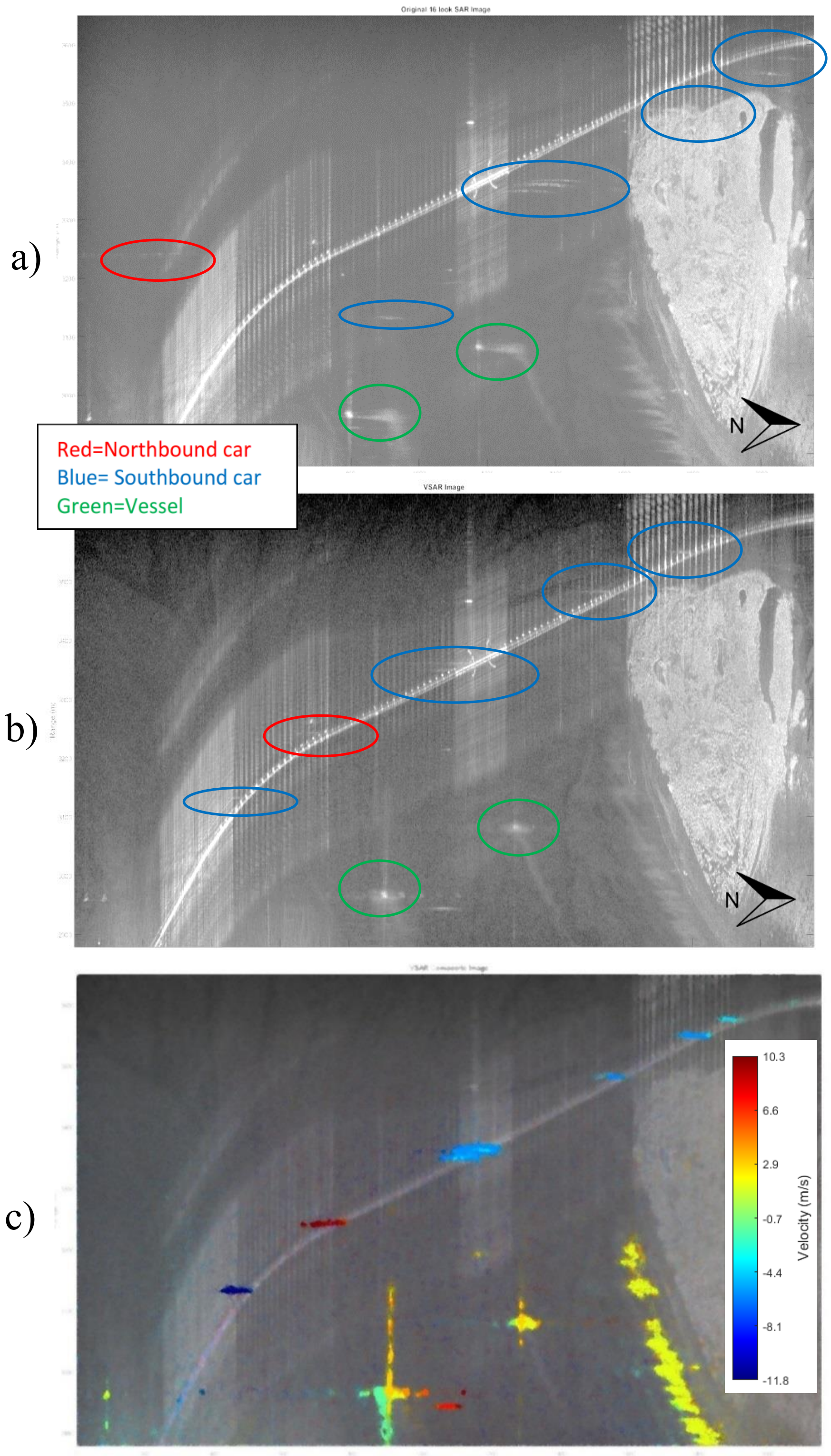

Figure 5. a) Uncorrected SAR image of the Oregon Inlet bridge with displaced cars and vessels highlighted. b) Corrected VSAR image, with vehicles moved back to bridge and vessels properly placed at the head of their signatures. c) Composite image, colorized by dominant velocity.

a)

b)

Figure 6. a) Uncorrected SAR image of shoaling waves and land near Oregon Inlet. b) Corrected VSAR image showing compressed shoaling wave signatures.

Figs. 6 and 7 illustrate VSAR's ability to correct the more complicated signatures that occur in maritime environments. In Fig. 6, the bright, horizontal streaks along the shore are shoaling waves. Due to crest acceleration, these signatures are spread in azimuth (the horizontal dimension in the image) through variation in the radial velocity found in (1). But VSAR corrects this distortion, producing signatures, seen in Fig. 6b, that more accurately represent the azimuthal extent of the waves. Fig. 7 demonstrates correction of a distorted vessel signature, produced by a small boat of opportunity. The uncorrected signature is shown in the top panel, while the lower image shows the signature after correction through VSAR processing. The improvement in fidelity is apparent. More detail on this correction can be found in [8], where the improvement in fidelity afforded by increasingly longer MSAR arrays is illustrated.

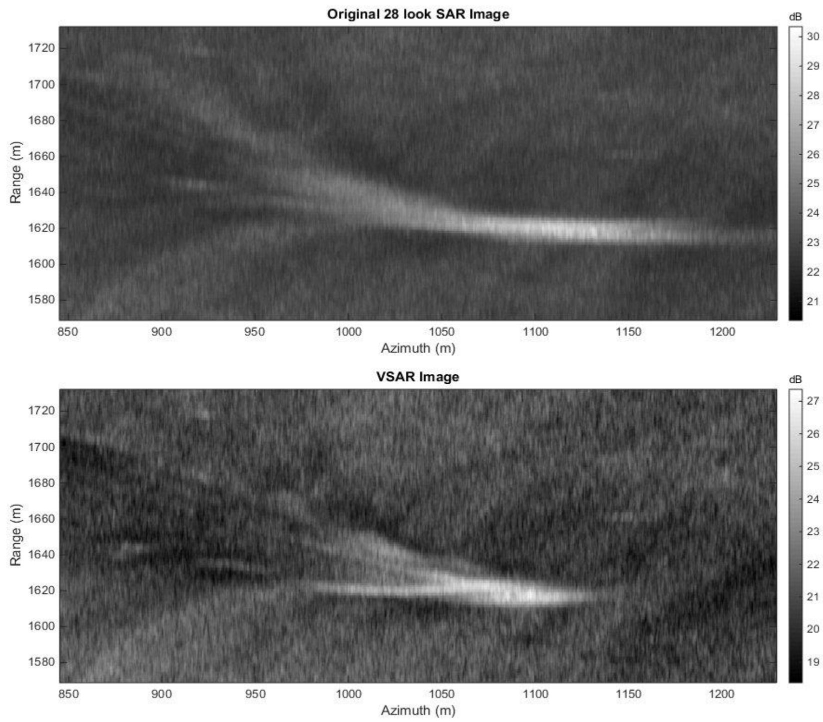

Figure 7. a) Signature of a moving boat, distorted due to complicated surface motion. b) Same boat signature after VSAR processing, with fidelity significantly restored.

5.0 CHANNEL BALANCING IN THE PRESENCE OF MULTIPATH

As discussed in [8], an adaptive algorithm is used to balance the magnitude and phase responses of the multiple channels in the NRL MSAR [9]. This operation is essential for effective VSAR processing, since without it, variations in the pixel phase along the time stack that are induced by the *radar system* will be erroneously interpreted as scene motion. If the scene is dominated by stationary objects, as is the case for a land image containing a few moving targets, this undesired phase variation can be determined from the imagery itself using the adaptive algorithm. The algorithm is also successful even for the maritime imagery presented in this paper, since the scenes contain stationary backscatter (generated by the coastline as well as the bridge) that is much brighter than that produced by the moving water and vessels. This bright backscatter drives the adaptive algorithm towards the correct solution. But if the scene contains only a dynamic ocean surface and possibly vessels moving on it, the averaging inherent in the algorithm will not (in general) produce the system-induced phase response, since the phase induced by wave motion will not (in general) average out. Thus, the adaptive balancing algorithm is not generally effective when applied to purely ocean scenes.

One potential approach to this problem is to measure the undesired, system-induced response using a stationary scene, then apply that correction to ocean-only imagery. For illustration, Fig. 8 shows the system-induced phase difference as a function of grazing angle for two pairs of phase centers, computed from NRL MSAR imagery of the Great Dismal Swamp in North Carolina, a uniformly forested region with little topographical relief. Each trace in the plots is produced by a 50-meter average in azimuth. (For the NRL MSAR, 32 plots such as those in Fig. 8 can be generated, one for each channel.) These phase oscillations with grazing angle are in all likelihood generated by multipath reflections off the aircraft fuselage and/or wings that mix coherently with the intended, direct-path signals from the scene [10] [11].

Potentially, the system response for all 32 phase centers could be computed using land-only data, then subsequently removed from all ocean-only imagery. However, these phase patterns vary between aircraft passes, sometimes significantly. This is illustrated in Fig. 9 which shows the responses for the same two phase centers, but computed from a pass over a different (flat) land scene. The shapes of the phase profiles differ from those in Fig. 8 as do the mean values (displayed as insets). This variation is possibly due to differences in aircraft attitude (in particular yaw) during the passes, differences that arise as the aircraft is trimmed to fly a prescribed path over ground in the presence of a prevailing wind. In simple multipath cases, modeling can be used to account for this variation [10] [11]. However, the profiles in Figs. 8 and 9 exhibit oscillations on both long and short (grazing angle) scales, indicating the presence of several multipath scattering centers on the aircraft. Efforts to fit parameters to the corresponding models are currently underway.

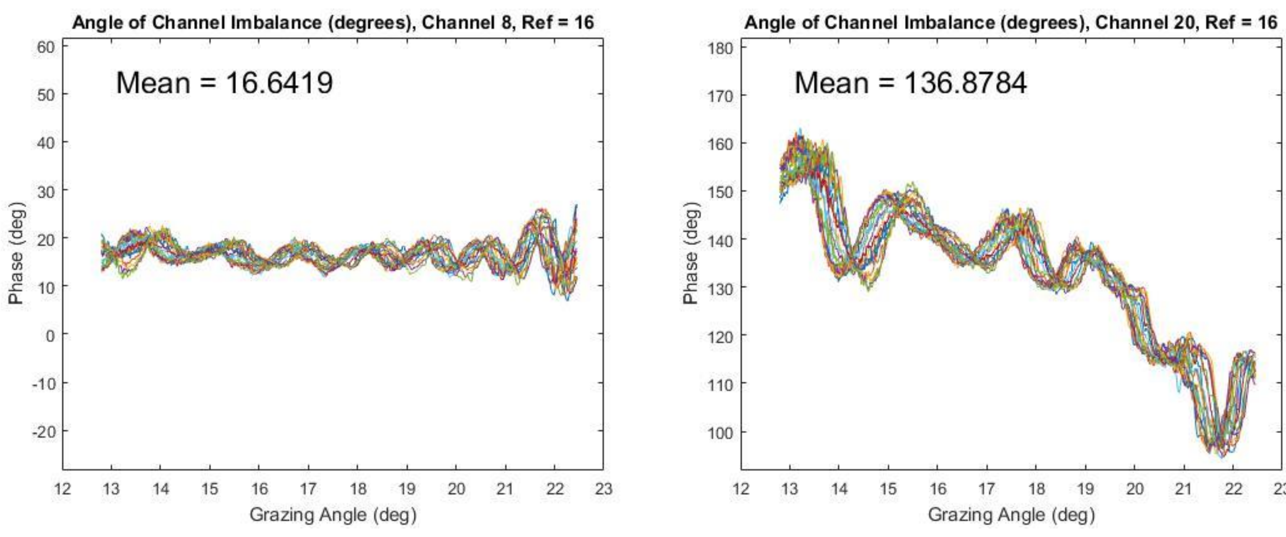

Figure 8. Phase response as measured from Great Dismal Swamp imagery a) Relative phase between the images from phase centers 8 and 16 as a function of grazing angle. b) Relative phase between the images from phase centers 20 and 16 as a function of grazing angle.

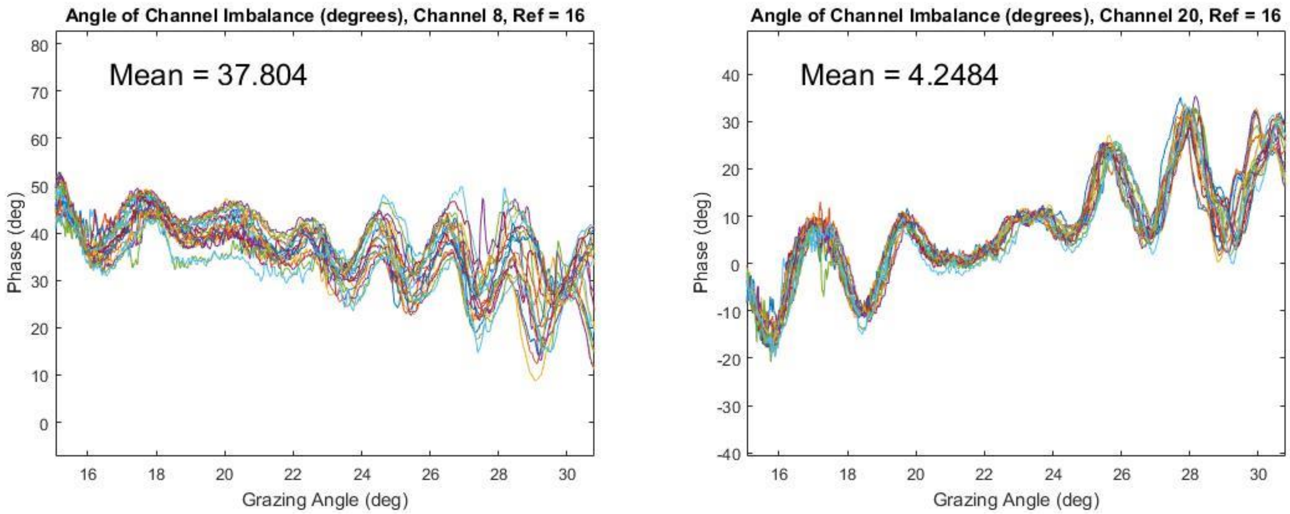

Figure 9. Same as Fig. 8, but computed using imagery a flat rural scene.

6.0 CONCLUSION

This paper describes the NRL MSAR and presents representative results that demonstrate the correction of image distortion induced by motion within the scene. These results demonstrate that VSAR can correct both the azimuthal displacements of discrete moving targets, such as automobiles, as well as the signature distortion induced by the more complex motion of maritime targets. Results are also presented that illustrate the challenge of balancing the phase response of the multiple channels in the presence of multipath reflection off the body of the aircraft.

References

[1] B. Friedlander and B. Porat, "VSAR: a high resolution radar system for detection of moving targets," IEE Proceedings - Radar, Sonar and Navigation, vol. 144, no. 4, pp. 205-218, 1997.

[2] B. Friedlander and B. Porat, "VSAR: a high resolution radar system for ocean imaging," IEEE Transactions on Aerospace and Electronic Systems, vol. 34, no. 3, pp. 755–776, July 1998.

[3] M. A. Sletten, "Demonstration of SAR distortion correction using a ground-based multichannel SAR test bed," IEEE Transactions of Geoscience and Remote Sensing, vol. 51, no. 5, pp. 3181–3190, May 2013.

[4] R. Jansen, M. Sletten, and R. Raj, "Performance Studies of emulated multichannel SAR for motion characterization", IEEE Transactions on Aerospace and Electronic Systems, Vol. 51, Issue 4, October 2015.

[5] Sletten, M., Menk, S., Toporkov, J., Jansen, B. and Rosenberg, L. "The NRL multi-aperture SAR system", International Radar Conference, Washington DC, USA, pp. 192-197, 2015.

[6] Sletten, M., Hwang, P., Toporkov, J., Menk, S., Rosenberg, L. and Jansen, B. “Analysis and correction of maritime signatures with the NRL MSAR”, IEEE International Conference on Geoscience and Remote Sensing, Milan, Italy, pp. 2489-2492, 2015.

[7] Rosenberg, L. and Sletten, M., “Analysis of maritime X-band velocity SAR imagery”, International Radar conference, Johannesburg, South Africa, pp. 121-126, 2015.

[8] Sletten, M. A., L. Rosenberg, S. Menk, J. Toporkov, and R. Jansen, “Maritime Signature Correction with the NRL Multichannel SAR”, to appear in the IEEE Transactions on Geoscience and Remote Sensing.

[9] C. H. Gierull, “Digital channel balancing of along-track interferometric SAR data,” DRDC Ottawa, Technical Memorandum, March 2003.

[10] M. Pinheiro, P. Prats, R. Scheiber, and J. Fischer, “Multi-Path Corrections Model for Multi-Channel Airborne SAR”, 2009 IEEE International Geoscience and Remote Sensing Symposium, Cape Town, South Africa, July 2009.

[11] Y. Mao, M. Xiang, L. Wei, and S. Han, “The Mathematical Model of Multipath Error in Airborne Interferometric SAR System” 2010 IEEE International Geoscience and Remote Sensing Symposium, Honolulu, HI, USA, July 2010.